independent variables (inoculums age, volume and concentration of sulphuric acid) and their interactions significantly influenced the hydrogen production. Optimum conditions optimized during the study were inoculums age, 21 h, inoculums volume, 50 ml/l and concentrations of sulphuric acid, 1.25%. Maximum bio-hydrogen production obtained with these optimum conditions was 705 ml. Results show that RSM (CCD) was a useful statistical tool for optimization of the key factors influencing the biohydrogen production.

Conflict of interest: No conflict of interest was declared.

Author's contribution: Veena Thakur and Mona Tandon were involved in modelling and designing of the experiment. Final manuscript drafting and compiling was done by S. K. Jadhav.

1. Fang, H. H. P., Zhu, H. G. and Zhang, T., Phototrophic hydrogen production from glucose by pure and co-cultures of *Clostridium butyricum* and *Rhodobacter sphaeroides*. *Int. J. Hydrogen Energ.*, 2006, **31**(115), 2223–2230.
2. Guragain, Y., Coninck, J. D., Husson, F., Durand, A. and Rakshit, S. K., Comparison of some new pretreatment methods for second generation bioethanol production from wheat straw and water hyacinth. *Bioresource Technol.*, 2011, **102**, 4416–4424.
3. Lin, C. Y., Lay, C. H., Sen, B., Chu, C. Y., Kumar, G., Chen, C. C. and Chang, J. S., Fermentative hydrogen production from wastewaters: a review and prognosis. *Int. J. Hydrogen Energ.*, 2012, **37**(2), 15632–15642.
4. Cheng, J., Su, H., Zhou, J., Song, W. and Cen, K., Hydrogen production by mixed bacteria through dark and photo fermentation. *Int. J. Hydrogen Energ.*, 2011, **36**, 450–457.
5. Gunnarsson, C. C. and Petersen, C. M., Water hyacinths as a resource in agriculture and energy production: a literature review. *Waste Manage.*, 2007, **27**(1), 117–129.
6. Moretti, M. M. *et al.*, Pretreatment of sugarcane bagasse with microwaves irradiation and its effects on the structure and on enzymatic hydrolysis. *Appl. Energy*, 2014, **122**, 189–195.
7. Zhang, H. and Wu, S., Dilute ammonia pretreatment of sugarcane bagasse followed by enzymatic hydrolysis to sugars *Cellulose*, 2014, **21**, 1341–1349.
8. Zhao, X., Xing, D., Fu, N., Liu, B. and Ren, N., Hydrogen production by the newly isolated *Clostridium beijerinckii* RZF-1108. *Bioresour. Technol.*, 2011, **102**(18), 8432–8436.
9. Zheng, Y., Zhao, J., Xu, F. and Li, Y., Pretreatment of lignocellulosic biomass for enhanced biogas production. *Prog. Energy Combust. Sci.*, 2014, **42**, 35–53.
10. Ma, F., Yang, N., Xu, C., Yu, H., Wu, J. and Zhang, X. Combination of biological pretreatment with mild acid pretreatment for enzymatic hydrolysis and ethanol production from water hyacinth. *Bioresour. Technol.*, 2010, **101**, 9600–9604.
11. Cheng, J., Su, H., Zhou, J., Song, W. and Cen, K., Hydrogen production by mixed bacteria through dark and photo fermentation. *Int. J. Hydrogen Energ.*, 2011, **36**, 450–457.
12. Zhang, J., Sun, H., Pan, C., Fan, Y. and Hou, H., Optimimization of process parameters for directly converting raw corn stalk to biohydrogen by *Clostridium* sp. FZ11 without substrate pretreatment. *Energy Fuels*, 2016, **30**(1) 311–317.
13. Kotay, S. M. and Das, D., Microbial hydrogen production with *Bacillus coagulans* IIT-BT S1 isolated from anaerobic sewage sludge. *Bioresour. Technol.*, 2007, **98**, 1183–1190.
14. Jaapar, S. Z. S., Mohd. Kalil, S, Ali, E. and Nurina, A., Effects of age of inoculum and headspace on hydrogen production using *Rhodobacter sphaeroides*. *Bacteriol. J.*, 2011, **1–8**.
15. Prakashan, R. S., Sathish, T. and Brahmaiah, P., Biohydrogen production process optimization using anaerobic mixed consortia: a prelude study for use of agro-industrial material hydrolysate as substrate. *Bioresour. Technol.*, 2010, **101**, 5708–5711.
16. Ferchichi, M. E., Crabbe, W., Hintz, G. H., Gil and Almadidy, A., Influence of culture parameters on biological hydrogen production by *Clostridium saccharoperbutylacetonicum* ATCC 27021 *World J. Microbiol. Biotechnol.*, 2005, **21**, 855–862.
17. Mannikadan, T. R., Dhanasekar, R. and Thirumavalan, K., Microbial production of hydrogen from sugarcane Bagasse using Bacillus sp. *Int. J. Chem. Technol. Res.*, 2009, **1**(2), 344–348.
18. Cheng, J., Lin, R., Song, W., Xia, A., Zhou, J. and Cen, K., Enhancement of fermentative hydrogen production from hydrolysed water hyacinth with activated carbon detoxification and bacteria domestication. *Int. J. Hydrogen Energ.*, 2015, **40**(6), 2545–2551.
19. Pattra, S., Sangyoka, S., Boonmee, M. and Reungsang, A., Sugarcane bagasse (SCB) used in hydrogen production by *Clostridium butyricum* was hydrolyzed using H_2SO_4 at various concentration. *Int. J. Hydrogen Energ.*, 2008, **33**(19) 5256–5265.

ACKNOWLEDGEMENT. We acknowledge Pandit Ravishankar Shukla University Raipur, Chhattisgarh, India, for providing the infrastructure and laboratory facility for the carrying out this work.

Received 25 February 2017; revised accepted 10 April 2017

doi: 10.18520/cs/v113/i04/790-795

Ionospheric precursors observed in TEC due to earthquake of Tamenglong on 3 January 2016

Sanjay Kumar and A. K. Singh*

Atmospheric Research Laboratory, Banaras Hindu University, Varanasi 221 005, India

Ground-based GPS data show the presence of earthquake precursor in the form of perturbation in TEC of the ionosphere. The analysis of data for Tamenglong Earthquake (M = 6.7, 3 January 2016) from the stations at Lhasa, China (29.65°N, 91.10°E), Hyderabad, India (17.41°N, 78.55°E), and Patumwan, Thailand (13.73°N, 100.53°E) for the duration of 5-days before and after the main shock of the earthquake show large enhancement and decease in TEC. The results for Lhasa station which lies in the Earthquake preparation zone showed a decrease in TEC on 29 December (–37%) and 30 December (–9%) which is followed by an enhancement in TEC (47%) on 31 December, i.e. 3 days before the main shock. After the

*For correspondence. (e-mail: abhay_s@rediffmail.com)

main shock negative ionospheric perturbation has been observed on 4, 5 and 7 January 2016 with a reduction of 20%, 32% and 24% respectively. Stations lying outside preparation zone (Patumwan and Hyderabad) did not show any ionospheric precursor.

Keywords: Earthquake, GPS TEC, ionosphere, seismo-electromagnetic.

EARTHQUAKE is the most terrifying and destructive natural phenomenon which leads to a great loss of human life, property and environment. To mitigate/minimize the loss, attempts are being made to find out ways and means for short-time/long-time predictions (Hayakawa[1]). Earthquake injects gases, particles, shock waves, electric field, etc. into the atmosphere/ionosphere which perturb different layers of the ionosphere[2–5]. The lithosphere–atmosphere–ionosphere interactions caused by seismic events have become important aspects for research.

Anomalies can be observed in different parameters of the ionosphere such as: plasma density, temperature, composition change and peak parameters of F2-layer (NmF2, foF2)[2–5]. In recent years due to the advent of global positioning system (GPS), total electron content (TEC) of ionosphere has become an important parameter and is widely used to observe the seismo-ionospheric anomaly. Reported results show positive as well as negative perturbations in TEC[3,6–8]. Emitted radon gas may ionize atmospheric constituents, whereas seismic originated electric field may cause plasma drift by $E \times B$ force. Namgaladze[9] considered $E \times B$ drift to be the most likely physical mechanism responsible for the seismo-ionospheric anomaly formation. Based on ground-based measurements, a significant decrease of the ionospheric electron density, foF2 and TEC simultaneously were observed 1–4 days before the Chi-Chi, Rei-Li and Chia-Yi earthquakes[2,10,11]. Recently, a case study and statistical analysis were made to observe pre-seismic anomalies in TEC[5,12–14].

In this communication, an effort has been made to identify ionospheric precursors in GPS-TEC data and discussed the mechanism of lithosphere–atmosphere–ionosphere coupling due to recent earthquakes at Tamenglong, India (24.8°N, 93.5°E). The main shock of this earthquake occurred at 23:05:16 UT on 3 January 2016. In the present study three GPS stations at Lhasa, Patumwan and Hyderabad were selected. The details of earthquake epicentre, radius of earthquake preparation zone, location of GPS stations, precursor days, etc. are summarized in Table 1.

GPS data with a time resolution of 30 sec were used. Lhasa GPS station lies within the circle of earthquake preparation zone at a distance of 589 km from the epicenter, whereas the other two stations (Patumwan and Hyderabad) are outside it. The slant total electron content (STEC) estimated from GPS data recorded in RINEX FORMAT is converted into vertical total electron content (VTEC)[15]. The hourly mean value of TEC has been used in this study. Data for five days before and five days after the earthquake were analysed. The statistical method described by Liu *et al.*[16] was used to separate anomalous variability arising due to earthquake from day-to-day variations in the ionosphere. In this method, standard deviation σ is used to specify the upper and lower inter quartile range (IQR) using the equations

$$\text{IQR upper bound (UB)} = \text{TEC(MM)} + 1.34\sigma, \quad (1)$$

$$\text{IQR lower bound (LB)} = \text{TEC(MM)} - 1.34\sigma, \quad (2)$$

where TEC(MM) is the monthly median of TEC data. The ionospheric perturbation has been divided into two categories: percentage increase and percentage decrease with respect to UB and LB respectively using the relations

$$\%\ \text{increase} = (\text{TEC} - \text{UB})/\text{UB} \times 100, \quad (3)$$

$$\%\ \text{decrease} = (\text{LB} - \text{TEC})/\text{LB} \times 100. \quad (4)$$

The changes in earth's crust in the form of deformations, variations in seismic waves, emanation of gases from the earth's crust, and changes in electrical conductivity were observed not only in the earthquake source region but also in the zone exceeding the source dimensions by an order of magnitude. Such a zone is called the earthquake preparation zone which is a circle (Figure 1) with a radius calculated using the relation[17]

$$\rho = 10^{0.43M}\ \text{km}, \quad (5)$$

where M is the magnitude of the earthquake.

The ionosphere is affected by so many parameters including solar and geomagnetic disturbances. Sometimes the phenomena in the lower atmosphere also play a significant role in ionospheric variations. In addition, ionosphere also shows diurnal, day-to-day, seasonal, spatial variations[18]. Therefore, the knowledge of background ionospheric condition is important to identify the ionospheric anomaly related to seismic activity. Figure 2 shows daily variations of D_{st}-index from 29 December 2015 to 9 January 2016. During the period, there was a geomagnetic storm ($D_{st} = -117$ nT) from 1200 UT, 31 December to 0100 UT, 01 January (Figure 2 *b*). Except for this period, the total considered period was quiet. Therefore any storm-induced disturbance in ionosphere can be expected only after 1200 UT on 31 December. In the case of intense geomagnetic storm, its impact on the ionosphere may remain for a day or more.

On 3 January 2016 a strong earthquake of magnitude 6.8 occurred at Tamenglong, Manipur, India at 23:05 UT h (04:30 LT on 4 January) (see Table 1). To

Table 1. Earthquakes of 3 January 2016 and effects on ionospheric perturbation observed from GPS and the IRI-2012 model

Earthquake date and epicenter	Radius of earthquake preparation zone (km)	Location of GPS observation stations	Distance of GPS station from the epicenter (km)	Ionospheric precursor observed in GPS-TEC
Tamenglong (Manipur) (24.8°N, 93.5°E) M = 6.7 Date: 03/01/2016 Time: 23:05:16 UT	761	Lhasa, China (29.65°N, 91.10°E)	589	3, 4, 5 d prior 1, 2, 4 d after
		Patumwan, Thailand (13.73°N, 100.53°E)	1433	1, 2 d after
		Hyderabad, India (17.41°N, 78.55°E)	1750	Same day

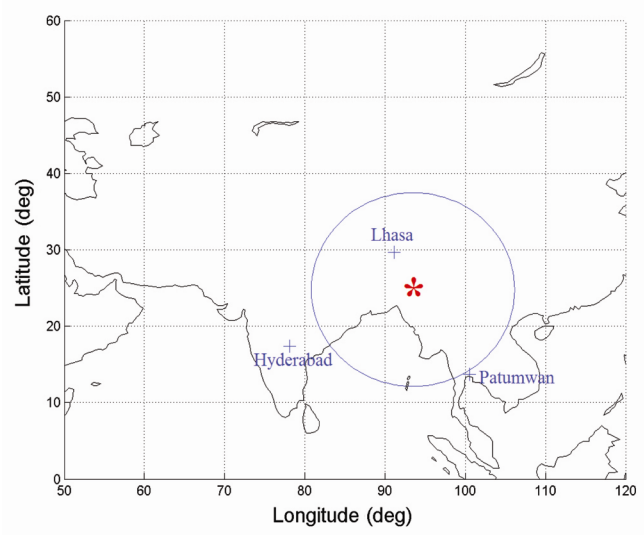

Figure 1. Map location of the earthquake epicenter (by *), and ionospheric measuring GPS station (by +). Circle indicates the earthquake preparation zone. The circle is plotted using the centre as epicentre of earthquake and radius computed by using formula $\rho = 10^{.43M}$ km.

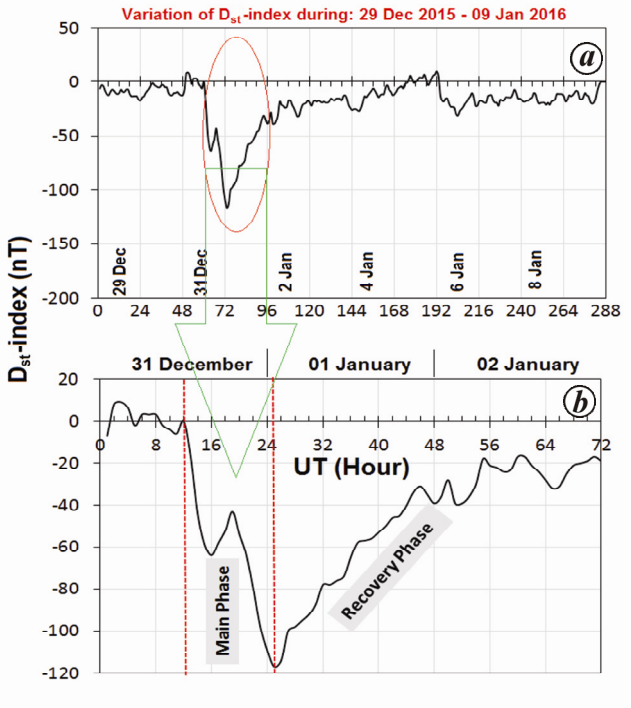

Figure 2. ***a***, Variation of D_{st}-index during 29 December 2015–9 January 2016. ***b***, Description of storm commenced on 31 December 2015.

study the impact of this earthquake, GPS-TEC values at EIA station Lhasa are plotted in Figure 3 for 11 days (5 days before and 5 days after the earthquake). To filter out the day-to-day variability of the ionosphere, UB and LB are also shown. In Figure 3, a strong ionospheric perturbation is observed with a reduction in TEC on 29 December (37%) and 30 December (9%) which is followed by an enhancement on 31 December 2015 (47% increase). This perturbation could not be attributed to the geomagnetic storm because its impacts on the ionosphere could only be felt after the commencement of the storm (i.e. 1200 UT, 31 December). Another enhancement in TEC (~70%) between 1400 and 1900 UT (i.e. after the storm commencement) has also been noticed from Figure 3, which may be due to the impact of geomagnetic storm. Therefore, the enhancement observed between 0400 and 1000 UT is totally free from the effect of geomagnetic storm and may be attributed to the earthquake. In order to confirm the association of this anomaly to the earthquake, the TEC variation on 31 December over other stations: Patumwan, Thailand (CUSV) and Hyderabad, India (HYDE), which were not within the circle of earthquake preparation zone, has been analysed (Figures 4 and 5). There was no significant enhancement in TEC during 0400–1000 UT on 31 December. The variation of TEC on 1–2 January does not show any significant ionospheric perturbation over Patumwan. On 3 January a small negative perturbation was observed (–22%). The ionospheric perturbation 5 days after the main shock (Figure 3 *b*) shows that the negative ionospheric perturbation was observed on 4, 5 and 7 January 2016 with a –20%, –32% and –24% respectively from the LB.

In this study an effort has been made to establish a connection between earthquake and anomaly observed in the TEC at low latitude station Lhasa lying in the preparation zone. Analysis showed the maximum ionospheric perturbation in TEC at LHAZ station at 1000 UT on 31 December which occurred before the storm

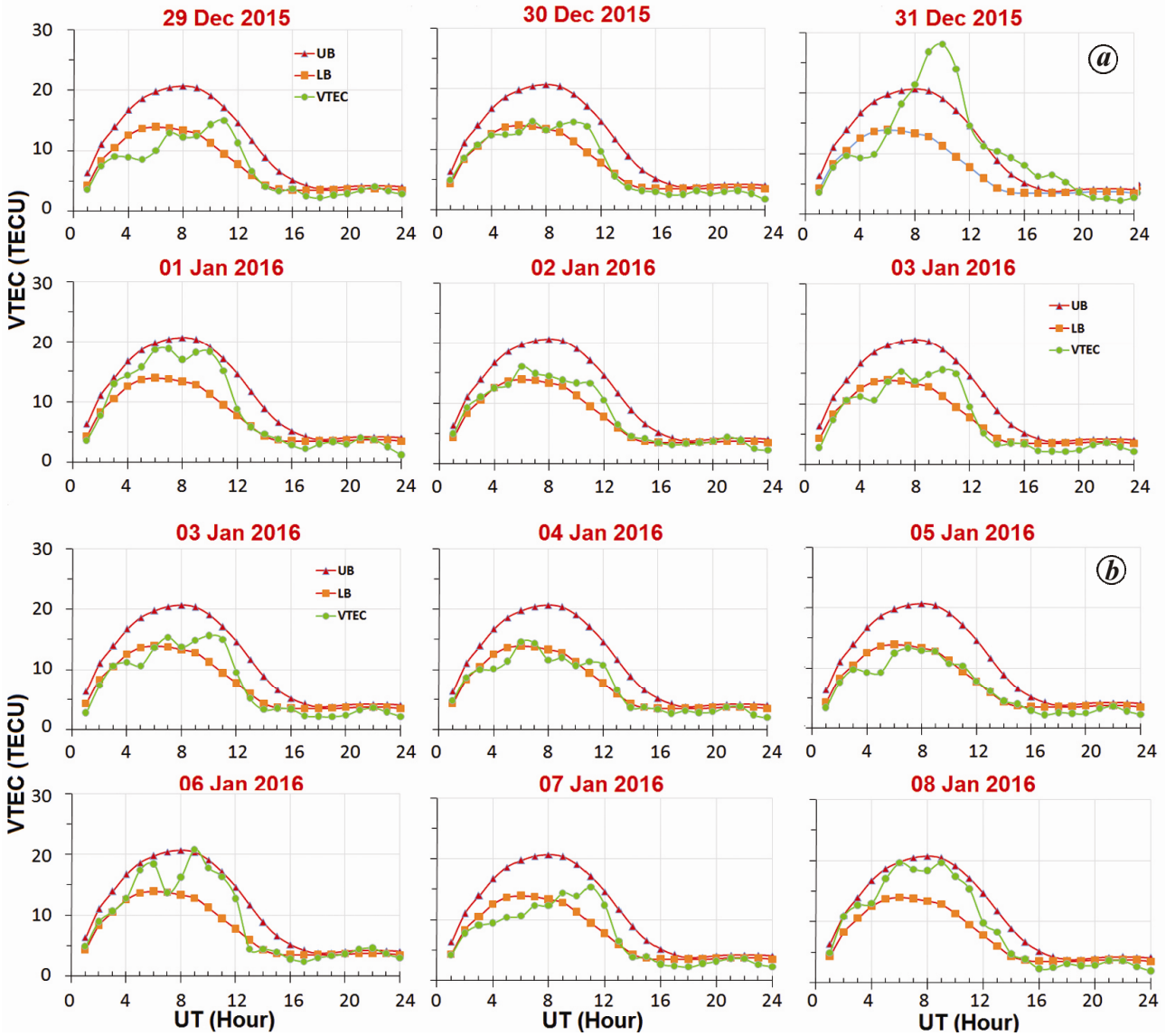

Figure 3. Variation of GPS-TEC along with upper bound (UB) and lower bound (LB) of interquartile range over Lhasa station. ***a***, 5 days before the main shock of earthquake. ***b***, 5 days after the main shock of earthquake.

commencement time 1200 UT, was totally free from the effect of geomagnetic storm. Therefore, the perturbation in GPS-TEC observed on 31 December 2015 can be considered as ionospheric precursor caused by the Earthquake. To ensure the presence of precursor in TEC values observed at LHAZ to be due to earthquake, TEC data at two more stations (Patumwan, Hyderabad) which are not lying inside the circle of earthquake preparatory zone were analysed; but no perturbation (enhancement) was observed during 0400–1000 UT on 31 December 2015.

The presence of precursor in GPS-TEC data was reported earlier[6–8]. However the magnitude of perturbation varied from case to case depending on the magnitude of earthquake and the distance of the observing station from the epicentre. Possible origins of pre-earthquake ionospheric anomalies have been discussed by several workers[19–21]. The source origin and the coupling mechanisms between the lithosphere, atmosphere and ionosphere are still not fully understood. Generally two well-known theories are proposed that can show connection between seismic activity and ionosphere. One mechanism relates to gravity wave generation and propagation up to the ionosphere altitude. The other mechanism is associated with the vertical electric field which links the earth with ionosphere[19]. In these two processes a physical connection between seismic activity and variations in ionosphere could be realized. The geoelectric signal generated by piezo-electric effect in seismically active region can modify atmospheric electric field and may play an important role in understanding the lithosphere–atmosphere–ionosphere coupling[20,21]. A large scale vertical electric field (~1000 mV m^{-1}) is supposed to be generated over the

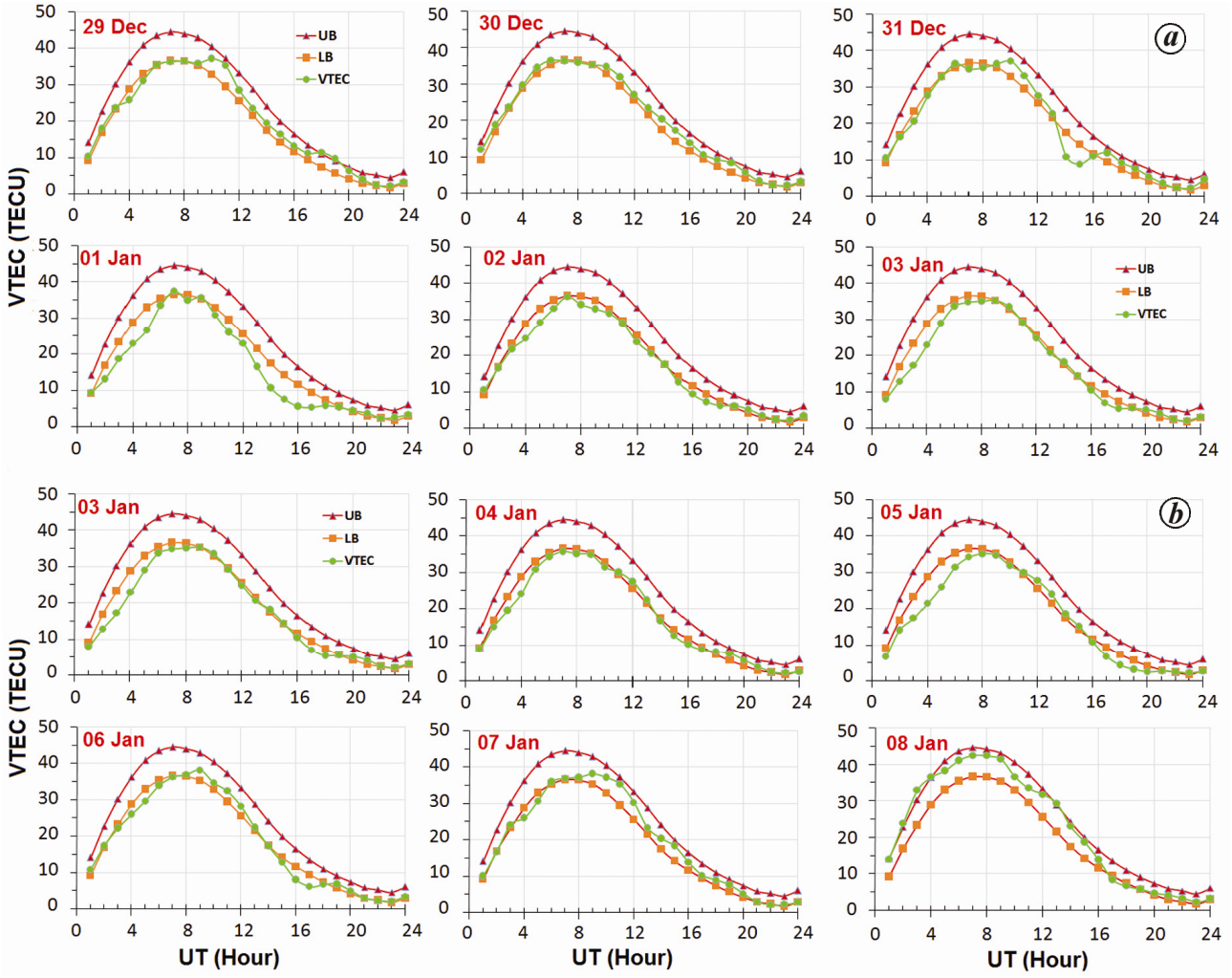

Figure 4. Same as Figure 3 but for Patumwan station.

active region a few days before the main shock of earthquake. This electric field can penetrate into the ionosphere and create perturbation in the electron density by $E \times B$ plasma drift mechanism[22]. In previous studies it was shown that seismic activity leads to an increase in the quasi-static electric field in the ionosphere which reaches ~10 mV/m, while its value on the earth's surface is ~100 V/m[23,24]. The field is localized in the ionosphere over the epicentre area, as well as, the related region with a characteristic horizontal scale of 100 to 1000 km depending upon magnitude of earthquake.

Theoretical calculations show that vertical electric field can penetrate into the ionosphere and can produce ionospheric perturbation when the area occupied by the electric field on the ground exceeds 200 km in diameter[22]. Using simulation results, Karpov *et al.*[25] showed that when seismic-induced electric current is directed towards the Earth, the resulting effect of the plasma drift components causes positive TEC disturbances to the east of the geomagnetic meridian of the epicentre, whereas a negative effect may occur to the west of the same. The opposite effects on TEC perturbations are attributed to change in the current/electric field direction in moving from east to west with respect to the geomagnetic meridian of the epicentre, which in turn affects the movement of the $E \times B$ plasma drift. Using ground and satellite-based measurements, anomalous changes starting from ground up to ionospheric levels for numerous earthquakes have been reported by several workers[5–8,19,26–28]. These studies show strong changes in various parameters on the surface and in the atmosphere/ionosphere a few days prior to the main shock of the earthquakes and provide strong evidences of lithosphere–atmosphere–ionosphere coupling.

In this study a connection between ionospheric anomaly (perturbation in TEC) and earthquake has been shown using data from GPS-based measurements over three stations: Lhasa, Hyderabad and Patumwan. The analysis of GPS-TEC data shows the appearance of a strong ionospheric precursor (enhancement by 47%) at Lhasa on 31 December 2015, i.e. 3-days before main shock of the earthquake. Stations lying outside the circle of earthquake preparation zone (Patumwan and Hyderabad) did

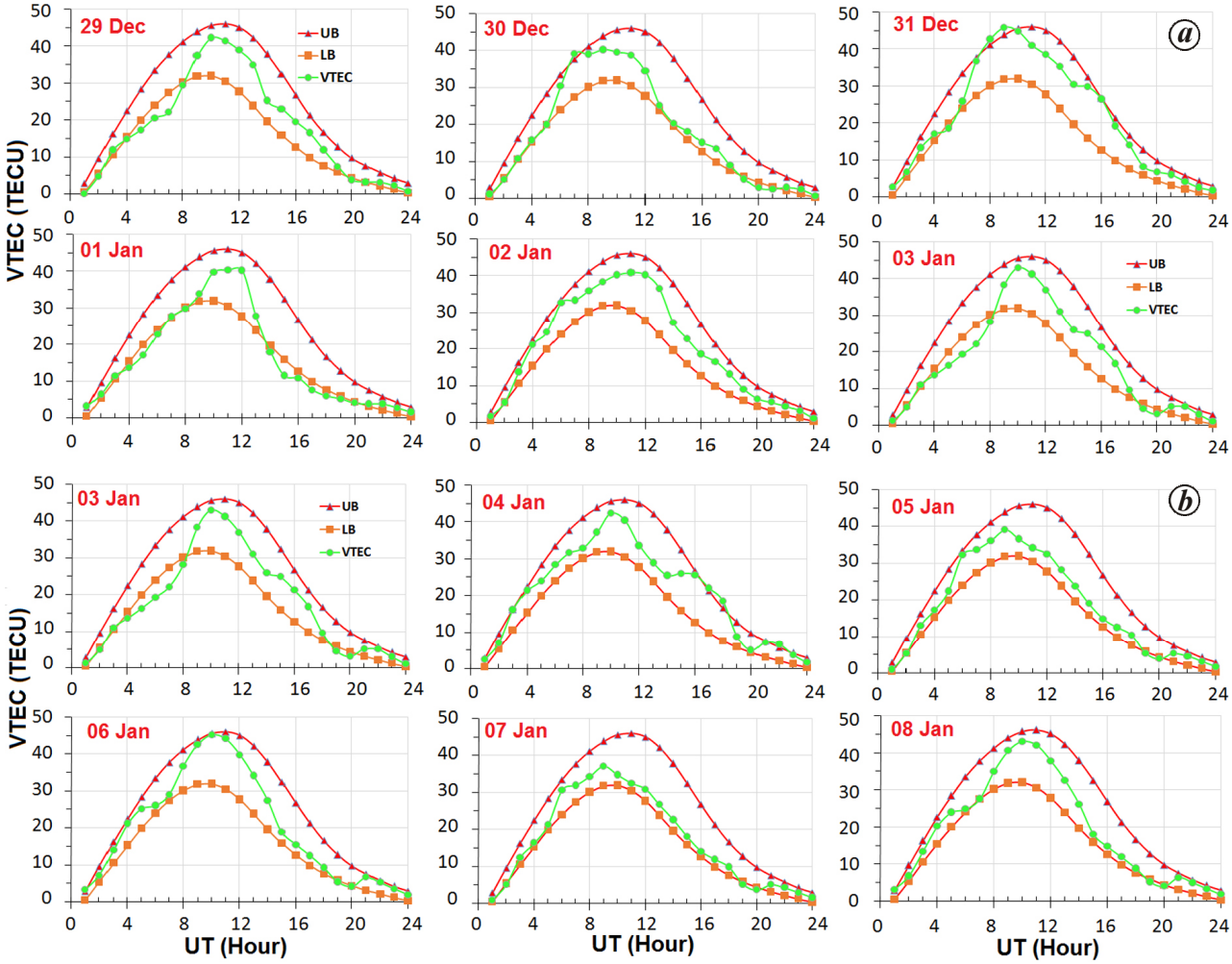

Figure 5. Same as Figure 3 but for Hyderabad station.

not show any precursor. A reduction in TEC was also observed on 29 (–37%) and 30 December (–9%), 2015.

It is important to note that during the period of data analysis, a geomagnetic storm occurred from 31 December 2015 to 1 January 2016, which commenced at 1200 UT on 31 December after the observed precursor in TEC. Any perturbation in ionosphere due to this storm was expected only after its commencement, i.e. 1200 UT on 31 December. Thus the observed ionospheric anomaly in GPS-TEC is totally free from the effect of this geomagnetic storm. However, an enhancement in TEC between 1400 and 1900 UT on 31 December 2015 has been observed which may be the impact of geomagnetic storm.

1. Hayakawa, M., VLF/LF radio sounding of ionospheric perturbations associated with earthquakes. *Sensors*, 2007, **7**, 1141–1158.
2. Liu, J. Y., Chen, Y. I., Chuo, Y. J. and Tsai, H. F., Variations of ionospheric total electron content during the Chi-Chi earthquake. *Geophys. Res. Lett.*, 2001, **28**, 1383–1386.
3. Sharma, K., Dabas, R. S., Sarkar, S. K., Das, R. M., Ravindran, S. and Gwal, A. K., Anomalous enhancement of ionospheric F2 layer critical frequency and total electron content over low latitudes before three recent major earthquakes in China. *J. Geophys. Res.*, 2010, **115**, A11313; doi:10.1029/2009JA014842.
4. Maurya, A. K., Singh, R., Veenadhari, B., Kumar, S. and Singh, A. K., Sub-ionospheric VLF perturbations associated with the 12 May 2008 *M* 7.9 Sichuan earthquake. *Nat. Hazards Earth Syst. Sci.*, 2013, **13**, 2331–2336.
5. Aggarwal, M., Anomalous changes in ionospheric TEC during an earthquake event of 13–14 April 2010 in the Chinese sector. *Adv. Space Res.*, 2015, **56**, 1400–1412.
6. Priyadarshi, S., Kumar, S. and Singh, A. K., Ionospheric perturbation in Total Electron Content (TEC) associated with two recent major earthquakes ($M > 5.0$). *Phys. Scr.*, 2011, **84**, 045901.
7. Priyadarshi, S., Kumar, S. and Singh, A. K., Ionospheric perturbations in total electron content (TEC) associated with some major earthquakes. *J. Geomantic Nat. Hazards Risk*, 2011, **2**(2), 123–139.
8. Li, J., Meng, G., Xinzhao, Y., Zhang, R., Hongbo, S. and Yufei, H., Ionospheric total electron content disturbance associated with May 12, 2008, Wenchuan earthquake. *Geodesy Geodyn.*, 2015, **2**, 126–134.
9. Namgaladze, A. A., Klimenko, M. V., Klimenko, V. V. and Zakharenkova, I. E., Physical mechanism and mathematical modeling of earthquake ionospheric precursors registered in total electron content. *Geomagnetism Aeronomy*, 2009, **49**(2), 252–262; doi:10.1134/S0016793209020169.

10. Liu, J. Y., Chuo, Y. J., Pulinets, S. A., Tsai, H. F. and Zeng, X., A study on the TEC perturbations prior to the Rei-Li, Chi-Chi and Chia-Yi earthquakes. In *Seismo Electromagnetics: Lithospheric–Atmospheric–Ionospheric Coupling* (eds Hayakawa, M. and Molchanov, O. A.), Terra Scientific, Tokyo, 2002, pp. 297–301.
11. Liu, J. Y. and Sun, Y. Y., Seismo-travelling ionospheric disturbances of ionograms observed during the 2011 *Mw* 9.0 Tohoku Earthquake. *Earth Planet. Space*, 2011, **63**, 897–902.
12. Liu, J. Y. *et al.*, Seismoionospheric GPS total electron content anomalies observed before the 12 May 2008 *Mw* 7.9 Wenchuan earthquake. *J. Geophys. Res.*, 2009, **114**, A04320; http://dx.doi.org/10.1029/2008JA013698.
13. Nishihashi, M., Hattori, K., Jhuang, H. K. and Liu, J. Y., Possible spatial extent of ionospheric GPS-TEC and NmF2 anomalies related to the 1999 Chi-Chi and Chia-Yi Earthquakes in Taiwan. *Terr. Atmos. Oceanic Sci.*, 2009, **20**, 779–789.
14. Sudarsanan, A. S., Bagiya, M. S., Reddy, C. D., Kumar, M. and Ramesh, D. S., Post-seismic ionospheric response to the 11 April 2012 East Indian Ocean doublet earthquake. *Earth Planet. Space*, 2015, **67**, 37.
15. Kumar, S. and Singh, A. K., Variation of ionospheric total electron content in Indian low latitude region of equatorial ionization anomaly (EIA). *J. Adv. Space Res.*, 2009, **43**, 1555–1562.
16. Liu, J. Y., Chuo, Y. J., Shan, S. J., Tsai, Y. B., Chen, Y. I., Pulinets, S. A. and Yu, S. B., Pre-earthquake ionospheric anomalies registered by continuous GPS TEC measurements. *Ann. Geophys.*, 2004, **22**, 1585–1593.
17. Dobrovolsky, I. P., Zubkov, S. I. and Myachkin, V. I., Estimation of the size of earthquake preparation zones. *Pure Appl. Geophys.*, 1979, **117**, 1025–1044.
18. Rama Rao, P. V. S., Gopi Krishna, S., Niranjan, K. and Prasad, D. S. V. V. D., Study of spatial and temporal characteristics of L-band scintillations over the Indian low-latitude region and their possible effects on GPS navigation. *Ann. Geophys.*, 2006, **24**, 1567–1580.
19. Liu, J. Y. and Sun, Y. Y., Seismo-travelling ionospheric disturbances of ionograms observed during the 2011 *Mw* 9.0 Tohoku Earthquake. *Earth Planet. Space*, 2011, **63**, 897–902.
20. Telesca, L., Colangelo, G., Hattori, K. and Lapenna, V., Principal component analysis of geoelectric signals measured in seismically active area of Basilicate Region (Southern Italy). *Nat. Hazards Earth Syst. Sci.*, 2004, **4**, 663–667.
21. Pulinets, S. and Ouzounov, D., Lithosphere–Atmosphere–Ionosphere Coupling (LAIC) model – a unified concept for earthquake precursors validation. *J. Asian Earth Sci.*, 2011, **41**, 371–382.
22. Pulinets, S. A., Legenka, A. D. and Zelenova, T. I., Dependence of the seismoionospheric variations in the *F*-layer maximum on the local time. *Geomag. Aeron.*, 1998, **38**, 400–402.
23. Sorokin, V. M. and Ruzhin, Y. Y., Electrodynamic model of atmospheric and ionospheric processes on the eve of an earthquake, *Geomag. Aeron.*, 2015, **5**(5), 626–642; doi: 10.1134/S0016793215050163.
24. Namgaladze, A. A. and Karpov, M. I., Conductivity and external electric currents in the global electric circuit. *Russ. J. Phys. Chem. B.*, 2015, **9**(4), 754–757; doi: 10.1134/S1990793115050231.
25. Karpov, M. I., Namgaladze, A. A. and Zolotov, O. V., Modeling of total electron content disturbances caused by electric currents between the earth and the ionosphere. *Russ. J. Phys. Chem. B.*, 2013, **7**(5), 594–598; doi:10.1134/S1990793113050187
26. Yasuoka, Y., Igarashi, G., Ishikawa, T., Tokonami, S. and Shinogi, M., Evidence of precursor phenomena in the Kobe earthquake obtained from atmospheric radon concentration. *Appl. Geochem.*, 2006, **21**, 1064–1072.
27. Singh, R. P., Mehdi, W. and Sharma, M., Complementary nature of surface and atmospheric parameters associated with Haiti earthquake of 12 January 2010. *Nat. Hazards Earth Syst. Sci.*, 2010, **10**, 1299–1305.
28. Sharma, K., Das, R. M., Dabas, R. S., Pillai, K. G. M., Garg, S. C. and Mishra, A. K., Ionospheric precursors observed at low latitudes around the time of Koyna earthquake. *Adv. Space Res.*, 2008, **42**, 1238–1245.

ACKNOWLEDGEMENTS. The work is financially supported by SERB, New Delhi under the Young Scientist Scheme (Project No. SR/FTP/ES-164/2014). The work is also partially supported by UGC, New Delhi under MRP Programme. The International GNSS Service (IGS) is thankful for providing GPS data which has been downloaded from website: ftp://cddis.gsfc.nasa.gov. We thank the World Data Center for Geomagnetism at Kyoto University Japan for providing geomagnetic data (http://swdcwww.kugi.kyto-u.ac.jp). We also thank Prof. R. P. Singh for his advice and improving this article.

Received 1 August 2016; re-revised accepted 19 April 2017

doi: 10.18520/cs/v113/i04/795-801